

# Diffusion-weighted magnetic resonance imaging for tumour response assessment: why, when and how?

A. Afaq, A. Andreou and D.M. Koh

Royal Marsden Hospital, Downs Road, Sutton, UK

Corresponding address: Dr Dow-Mu Koh, Royal Marsden Hospital, Downs Road, Sutton, SM2 5PT, UK.

Email: dowmukoh@icr.ac.uk

## Abstract

Diffusion-weighted magnetic resonance imaging (DWI) is increasingly being used to assess tumour response to a variety of anticancer treatments. The technique is quick to perform without the need for administration of exogenous contrast medium, and enables the apparent diffusion coefficient (ADC) of tissues to be quantified. Studies have shown that ADC increases in response to a variety of treatments including chemotherapy, radiotherapy, minimally invasive therapies and novel therapeutics. In this article, we review the rationale of applying DWI for tumour assessment, the evidence for ADC measurements in relation to specific treatments and some of the practical considerations for using ADC to evaluate treatment response.

**Keywords:** *Diffusion-weighted magnetic resonance imaging; tumour response; anticancer treatments.*

## Introduction

The ability to detect tumour response at an early stage of treatment is desirable in cancer imaging. As each patient and tumour is unique, accurate assessment of response at an early stage may allow modification of treatment by intensifying therapy in non-responders with the aim of improving clinical outcome; or early termination of ineffective treatment to avoid unnecessary drug toxicity.

In drug development, detection of drug effects on tumours in early phase clinical trials aids understanding of the mechanistic actions of drugs, and can help in determining a biological active drug dose for subsequent application. In this way, the efficiency of drug development may be enhanced by accelerating the research on drugs that demonstrate early efficacy, and halting the development of inefficacious or toxic therapies.

## Limitations of current imaging for tumour response assessment

In oncology, despite the advent of many new targeted therapies, tumour size measurements before and after treatment remain the most widely used and accepted method for evaluating tumour response to treatment. The first set of guidelines for assessing tumour regression

by measuring bi-dimensional tumour diameters before and after therapy, were first proposed by the World Health Organization (WHO) in 1979<sup>[1]</sup>. These were modified and simplified as the Response Criteria In Solid Tumours (RECIST) criteria in the 1990s, whereby only the maximum tumour diameter was considered<sup>[2]</sup>. The RECIST criteria were further streamlined in 2009, and the current version 1.1 remains the principle basis by which tumour response to a range of anticancer treatments are assessed<sup>[3]</sup>. However, reduction in tumour diameter usually occurs late in the course of treatment (typically 6–12 weeks), and is thus relatively insensitive to early treatment effects.

In recent years, the accelerated discovery of anticancer drugs has led to emergence of new therapies that are targeted towards specific cancer cell growth or metabolic pathways rather than being cytotoxic. Many of these drugs can be clinically effective but may not result in significant reduction in tumour size. Thus, assessing the effectiveness of such treatments by applying RECIST measurement criteria may be inaccurate or erroneous in categorizing treatment response<sup>[4]</sup>.

There are other potential limitations of adopting the RECIST criteria. First, even if there is a reduction in tumour size, this may not necessarily translate to improved survival for the patient, which is often the end point used for assessing drug efficacy. Second,

RECIST criteria cannot be used to objectively measure certain types of malignant involvement, such as metastases confined to bones or diffuse peritoneal infiltration. Third, tumour size measurements may be prone to errors, such as when a lesion is ill-defined or non-uniform in shape<sup>[5]</sup>.

For these reasons, imaging criteria apart from tumour size measurement are being developed to refine response assessment. For example, in the evaluation of patients with gastrointestinal stromal tumour (GIST) treated with the drug imatinib, one study has shown that using a combination of imaging criteria, including a 10% decrease in unidimensional tumour diameter and a 15% decrease in the computed tomography (CT) density value, resulted in better classification of responders from non-responders; with responders also showing longer progression-free survival<sup>[6]</sup>. Such an approach is now being tested in a multi-centre setting.

## Functional imaging techniques

Functional imaging has emerged as an important development in the past decade. Using functional magnetic resonance imaging (MRI), CT, ultrasound and radionuclide techniques, patho-physiological alterations in tissue vascularity, elasticity, metabolism, hypoxia and tissue water diffusivity can be measured and quantified. Of these, measurement of tumour metabolism, vascularity and water diffusivity have been applied for assessing tumour response to anticancer treatment.

Considering metabolic activity, [<sup>18</sup>F]fluorodeoxyglucose (FDG) positron emission tomography (PET) and now FDG PET/CT utilizes the increased glucose uptake by tumour tissue as an objective measure of tumour metabolism. By comparing the degree of tracer uptake on sequential studies before and after treatment, tumour response can be determined. The technique is already in routine clinical use for a variety of cancers, including head and neck, oesophageal, lung, colorectal and cervical cancers, as well as lymphomas. However, the technique is not without its limitations, as tumours with small metabolic dimensions may still be missed, and certain tumour types may not demonstrate increased glucose metabolism (e.g. neuroendocrine, prostate and bronchoalveolar cell carcinomas)<sup>[7]</sup>.

Metabolic activity can also be evaluated using proton MR spectroscopy (<sup>1</sup>H-MRS). For example, in the prostate gland, increased metabolite ratios of choline relative to citrate on <sup>1</sup>H-MRS is seen in tumours; and the reversal of this ratio or metabolic atrophy of choline levels could act as a marker of treatment response<sup>[8,9]</sup>. However, the implementation of <sup>1</sup>H-MRS requires substantial technical support, which may not be widely available. A recent meta-analysis also suggests that <sup>1</sup>H-MRS may have limited accuracy in identifying foci of prostate cancer in multi-institutional studies, highlighting the challenges of translating such a technique to a wider setting<sup>[10]</sup>.

Quantitative indices that reflect tumour vascularity can be derived with dynamic contrast-enhanced (DCE) ultrasound (US), DCE CT and DCE MRI. The change in signal intensity or enhancement of the tumour tissue after contrast administration is used to mathematically derive quantitative vascular parameters. For example, using DCE MRI, one of the most frequently derived parameters is the transfer constant  $K^{trans}$ , which reflects both blood flow and microvessel permeability. These techniques have been used to evaluate the effects of drugs that modulate tumour vasculature, such as anti-angiogenic and antivascular treatments<sup>[11]</sup>.

## Diffusion-weighted MR imaging (DWI) for assessing tumour response

### *Why?*

DWI is unique among imaging techniques as the image contrast and tissue quantification is based on differences in the mobility of water protons between tissues. No other current imaging technique provides insight into this aspect of the tissue microenvironment. Although many studies have confirmed the usefulness of DWI in a diagnostic role in cancer imaging, a significant and growing volume of data are now gathering to support its use for tumour response assessment<sup>[12]</sup>.

In the body, thermally driven motion (diffusion) of water molecules is impeded to different extents, depending on the environment within which these molecules reside. In tissues with high cellularity (e.g. tumour tissue), the motion of water protons are more impeded by barriers imposed by cell membranes, macromolecules and tortuosity of the extracellular spaces. An area with impeded water diffusion will appear as high signal on DWI images and return low apparent diffusion coefficient (ADC) values. Not surprisingly, tumour tissues often return lower ADC values compared with normal tissues<sup>[13]</sup>.

When tumours are treated by a range of anticancer therapies (e.g. chemotherapy, radiotherapy, radiofrequency ablation, cryoablation, embolization and targeted novel therapies), treatment-induced cell death by apoptosis, necrosis and cell lysis will lead to an increase in the mobility of water in the tissue microenvironment. This increase in water diffusion translates to an increase in the measured tissue ADC (Fig. 1). Thus, by quantifying tumour ADC before and after anticancer therapies, tumour response or lack of response to treatment can be determined. Studies in animals and humans in a variety of tumour types have shown that successful anticancer therapy results in an increase in the measured tumour ADC. ADC increase in tumour tissues after treatment has been shown to correlate with pathological changes including necrosis and apoptosis<sup>[14]</sup>.

Some of the perceived advantages of using DWI for assessing tumour response are that it is relatively quick

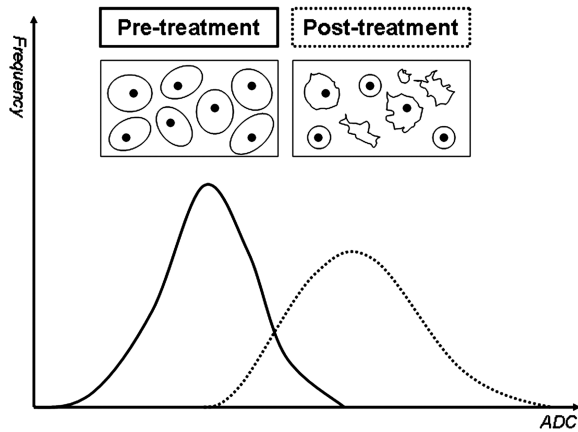


**Figure 1** Schematic diagram showing ADC changes with anticancer treatment. Graphs show frequency plots of ADC values in tumours before (solid black line) and after (dotted black line) therapy. Inserts depict a cluster of tumour cells, which demonstrate cellular lysis and apoptosis following treatment, thus increasing the mobility of water protons in that microenvironment. Note that successful therapy results in a shift of the ADC frequency plot (dotted line) towards the right as a result of increasing ADC values.

and easy to perform (typical imaging time of 1–5 min), does not require the administration of exogenous contrast material and results in a biologically relevant quantified parameter, ADC. Another important factor that merits consideration is that ADC measurements, in a well-conducted study, appear to be highly reproducible. In a two-centre clinical trial setting, the coefficient of variance for ADC measurement in the body was approximately 7% (coefficient of repeatability 14%)<sup>[15]</sup>. In another study to address measurement variability between scanners, the coefficient of variance of ADC measurements in the brain of normal volunteers was also found to be about 7%<sup>[16]</sup>. This means that although ADC increase may not be specific to the type of therapy administered, there can be some confidence in using the technique to detect a relatively small percentage increase in ADC values, increasing the likelihood of observing a significant drug effect.

### When?

Changes in tumour ADC measurements often precede any measurable change in tumour size or volume. Hence, determination of ADC response may influence clinical practice by allowing much earlier adjustments in therapy. Temporal evolution of ADC within tumour tissue to therapy has been shown to vary to some extent according to tumour type and the nature of treatment administered.

In theory, tumour ADC increases after initiating treatment because of cellular damage leading to tumour lysis, loss of cell membrane integrity and apoptosis; thus

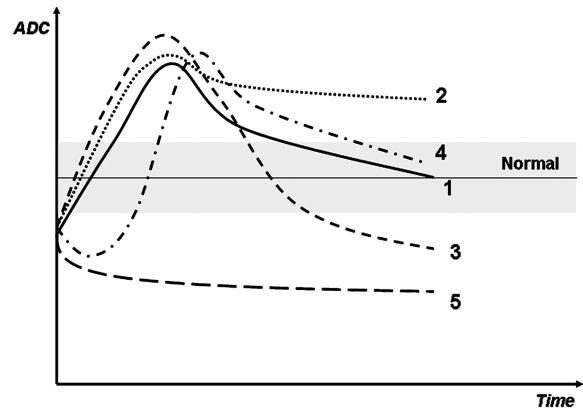


**Figure 2** Diagram showing theoretical changes in the ADC values of tumours after commencing anticancer therapy. Plots demonstrate possible evolutions of tumour ADC ( $y$ -axis) with time ( $x$ -axis). Horizontal line and grey bars across the centre of the graph indicate the median ADC of normal tissue and the associated variability (95% confidence limits). Tumours typically return lower ADC than normal tissues. However, after commencing treatment, tumour ADC in responders rises to a peak and then gradually decreases to normal values in tissue (line 1). In some scenarios, there may be an increase in ADC that is sustained over a long period of time after treatment (line 2). In others, there may be an initial increase in ADC but a subsequent decrease that dips below the anticipated normal range (line 3). This ADC reduction may be attributed to fibrosis or inflammatory response. In addition, the ADC value may initially decrease before increasing with further therapy (line 4). In non-responders, there is often no change in the tumour ADC values. However, tumour growth or disease progression can lead to further ADC reduction (line 5).

increasing the mobility of water in the tissue microenvironment. However, acute cellular swelling as a result of treatment can lead to a transient decrease in ADC value<sup>[17]</sup>. The post-treatment increase in ADC value should normalize and decrease with time towards that of normal tissue as cancer cells are destroyed. Tumour re-growth could lead to further reduction in the ADC value (Fig. 2). However, deviation from this simplified schema can result from specific therapies, and also from tissue responses such as inflammation, fibrosis and fat infiltration, which can modify the ADC evolution<sup>[18,19]</sup>.

What has been consistently shown in the published literature is that ADC increase can be observed in response to a range of anticancer therapies within 30 days of initiating treatment in many cancers (Fig. 3). In cervical, rectal, head and neck cancers and liver metastasis, an increase in ADC has been reported within the first 2 weeks after the start of chemotherapy or radiotherapy. However, in some studies<sup>[20]</sup>, ADC increases were investigated and reported at later imaging time points (e.g. at 3 months or beyond). Despite the considerable variability in the timing of ADC investigations in relation

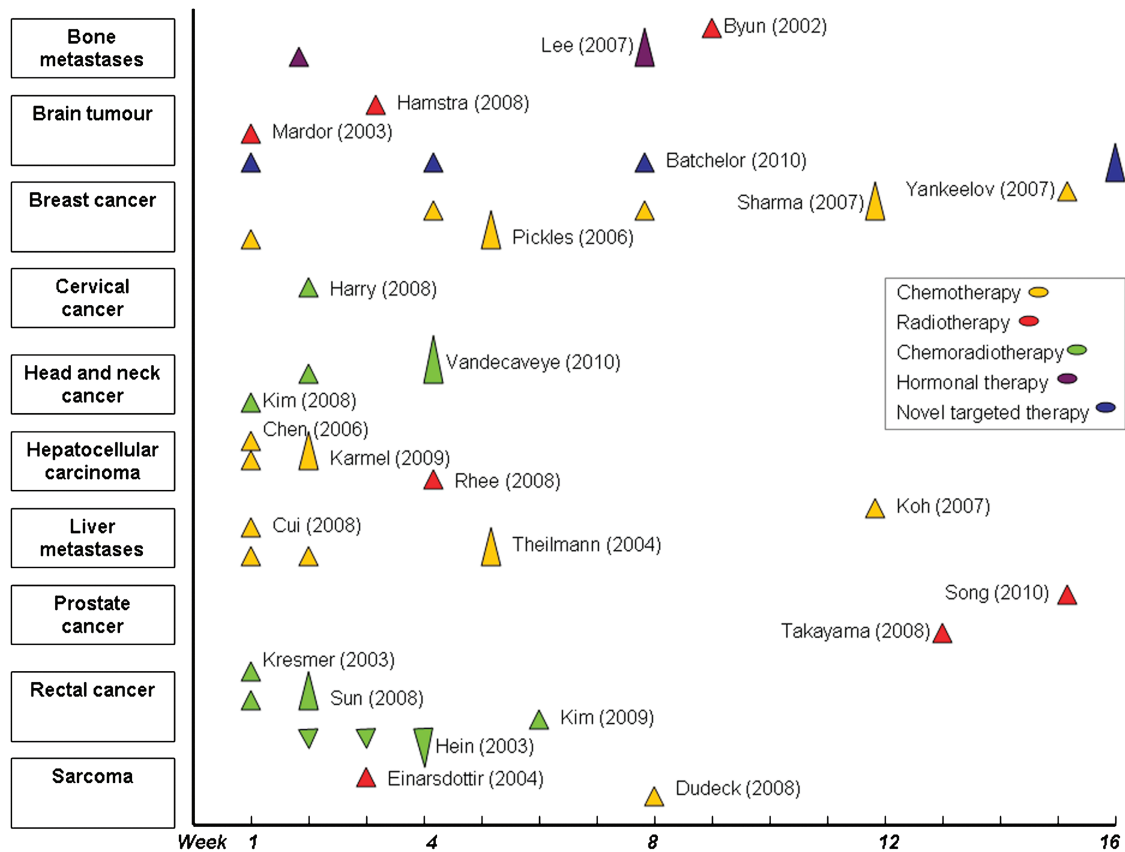


**Figure 3** Chart summarises published studies using ADC values to assess tumour response to chemotherapy (yellow), radiotherapy (red), chemoradiotherapy (green), hormonal therapy (purple) and targeted treatment (blue). The vertical axis shows tumour types and the horizontal axis indicates the timing of ADC measurements (in weeks) after starting treatment. Each study is displayed across from top to bottom according to tumour types and indicated on the chart (author, year). Upward arrowheads indicate an increase in ADC and downward arrowheads indicate a decrease in ADC. In studies in which multiple ADC measurements were taken, larger symbols indicate maximum ADC change. Note that many studies showed an increase in ADC values within 4 weeks of treatment. Furthermore, a number of studies showed a significant increase in ADC values within 1 week of commencing therapy.

to therapy reported in the literature, ADC still appears to be a potentially useful response biomarker in cancer treatment.

### Chemotherapy

Chemotherapy-induced increases in ADC values have been observed from within 3 to 90 days of initiating treatment (Fig. 4). This relatively large window of ADC increase is likely to reflect the duration of chemotherapy (typically 3–4 months) with sustained cytopathic effects. It would appear that measuring ADC increase within the first or second cycle of chemotherapy may also be prognostic in some tumour types, as patients showing increases in ADC values in this period were more likely to be responders defined by conventional size measurement criteria at the end of treatment. One of the areas of continuing investigation is the ADC evolution in residual abnormalities after chemotherapy; and the degree to which ADC can distinguish between residual disease and post-treatment change.

There is early evidence to suggest that continued impeded diffusion within an area of treated tumour can help to identify residual disease<sup>[21]</sup>.

Treatment response in bone metastases merits separate consideration as the normal bone marrow in adults contains substantial amounts of fat-containing yellow marrow, which normally returns very low ADC values (typically  $<0.5 \times 10^{-3} \text{ mm}^2/\text{s}$ ). Thus, unlike most soft tissues, metastatic and infiltrative malignant diseases will return ADC values that are higher than that of normal bone marrow but overlap with ADC values of red marrow<sup>[22]</sup>. Effective treatment results in further increase in ADC values, but subsequent bone remodeling and fat repopulation of treated disease leads to return of very low ADC values.

### Radiotherapy

In studies evaluating the effects of radiotherapy, increased ADC values in treated tumours have been reported from 1 week to about 4 months<sup>[23]</sup> after

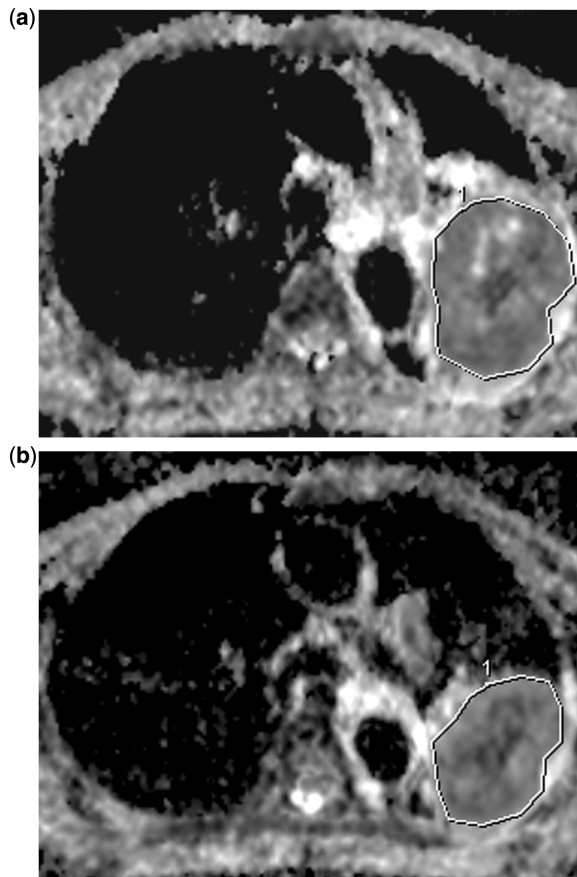


**Figure 4** ADC maps in a man with non-small cell lung cancer (a) before and (b) after 1 month of chemotherapy. Following treatment, there was a 20% increase in the median ADC value of the tumour (pre-treatment  $0.9 \times 10^{-3} \text{ mm}^2/\text{s}$ , post-treatment  $1.1 \times 10^{-3} \text{ mm}^2/\text{s}$ ) within the ROIs drawn (outlined) in keeping with the treatment effects. The patient was classified as a responder at 12 weeks after completing chemotherapy by conventional size criteria.

initiating therapy. The earliest increase in ADC at 1 week has been observed in brain tumours<sup>[24]</sup> consistent with radiation damage; and early increase in ADC within 3 weeks of treatment was shown to correlate with better clinical outcome<sup>[25]</sup>. Radiotherapy has also been combined with chemotherapy for the treatment of cervical, head and neck and rectal cancers. In these tumours, early ADC increases were observed within 1–2 weeks of initiating chemoradiotherapy, but it was not possible to isolate the relative contributions of radiotherapy versus chemotherapy to the ADC changes.

It is well known that radiation induces a fibrotic response in extracranial soft tissues that can contain variable degrees of inflammatory infiltrates, thus modulating the ADC evolution. The effects of fibrosis on ADC values of tumours in the body have not been fully characterized. One study in rectal cancer<sup>[26]</sup> showed

progressive reduction in ADC values following chemoradiotherapy at 4 weeks after treatment, which was ascribed to cytotoxic oedema and onset of fibrosis. In another study by Kim *et al.*<sup>[27]</sup> evaluating ADC values in patients with rectal cancer after completion of chemoradiotherapy, it was found that complete responders had significantly higher ADC values compared with non-complete responders, even though fibrosis was likely to be present at the site of treated disease amongst the complete responders. Hence, it appears that radiation-induced fibrosis can return relatively high or low ADC values, which may be related to the associated inflammatory infiltrates, tissue oedema and the nature of the collagen and fibroblastic response. Furthermore, radiation-induced changes may be sustained, as has been shown by the slow resolution of such changes on conventional imaging in a variety of clinical scenarios. Further work is required to correlate ADC measurements with tissue fibrosis at histopathology following radiotherapy. However, in an area of treated disease, a focal area of progressive ADC reduction should still raise the suspicion of disease recurrence (Fig. 5).

### Minimally invasive therapies

ADC increase in hepatocellular carcinoma (HCC) was reported as early as 2 days after transcatheter arterial chemoembolization (TACE)<sup>[28]</sup>. In one well-conducted study in patients with HCC, TACE treatment resulted in immediate reduction in arterial perfusion but ADC was only significantly increased at 1–2 weeks after treatment. In another study, an increase in ADC was observed in HCC treated with yttrium-90 radioembolization at 1 month after treatment<sup>[29]</sup>. Following radiofrequency ablation of liver metastases, ADCs of ablative zones were found to be higher than those of normal liver at 4 weeks after treatment in keeping with tissue necrosis.

### Novel therapeutics

Novel targeted therapeutics act via specific pathways to arrest tumour growth or induce tumour cell death. The differing mechanistic actions of these drugs can lead to differences in ADC response. For example, in one study evaluating the anti-angiogenic drug cediranib in patients with glioblastoma, vascular normalization induced by the drug resulted in alleviation of tumour-associated vasogenic oedema, leading to ADC reduction in the brain<sup>[30]</sup>. Alleviation of oedema has been shown to correlate with clinical improvement even though there may be further tumour infiltration into the white matter as shown by a further decrease in ADC<sup>[31]</sup>. In another study of HCCs treated using the anti-angiogenic drug sorafenib<sup>[32]</sup>, ADC reduction was initially observed in the first week after treatment, which was ascribed to haemorrhage, after which an increase in ADC was observed in keeping with anti-tumour effects.

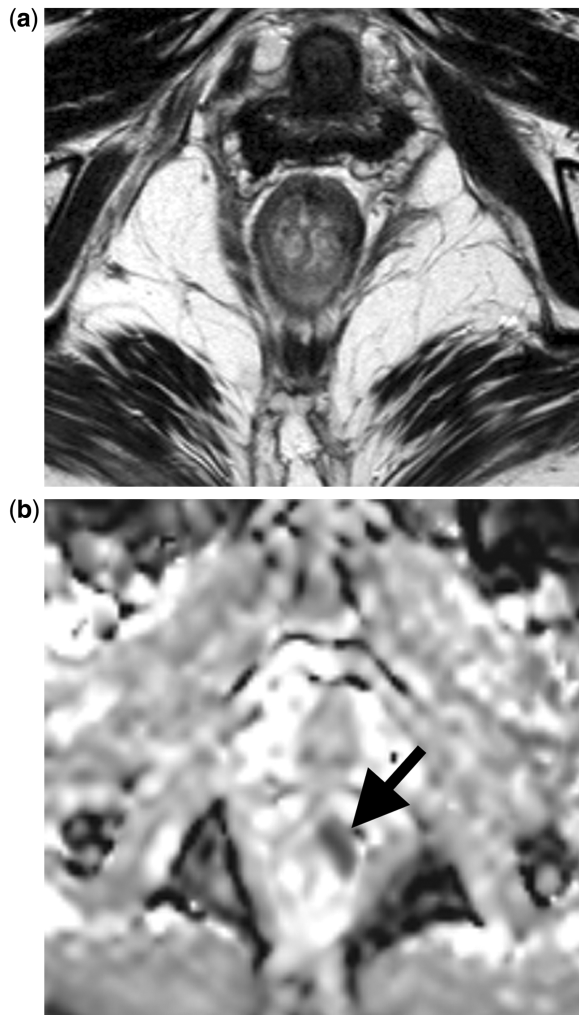


**Figure 5** A middle-aged woman with rectal cancer who showed complete response to chemoradiotherapy. (a) On follow-up MRI, a T2-weighted MR image showed no apparent abnormality in the rectal wall. (b) An ADC map revealed a crescent of impeded diffusion with low ADC values in the left rectal wall (arrow). Biopsy confirmed disease recurrence.

ADC was also used to evaluate the effects of treatment with the antivascular drug, combretastatin A4 phosphate. It was found that the second dose of treatment appeared to be more effective than the first in inducing significant increase in ADC<sup>[15]</sup>. It is possible that the first dose of an antivascular treatment results in areas of necrosis within a tumour, making it more susceptible to the effects of the second dose.

### Predicting response using pre-treatment ADC values

One of the most intriguing findings of using DWI for cancer assessment is that the pre-treatment ADC measurements may predict response of tumours to anticancer

therapies. Studies in rectal carcinoma<sup>[33–35]</sup>, cerebral gliomas<sup>[36,37]</sup>, colorectal and gastric hepatic metastases<sup>[14,38]</sup> have shown that tumours with low baseline pre-treatment ADC values respond better to chemotherapy/radiotherapy treatment compared with tumours that exhibit high pre-treatment ADC values. Higher ADC values are observed in necrotic tissue and in tissue with loss of cell membrane integrity. Before treatment, the presence of these changes may indicate a more aggressive phenotype. Regions of necrosis within a tumour are often hypoxic, acidotic and poorly perfused, resulting in diminished sensitivity to chemotherapy and radiotherapy. However, the pre-treatment ADC values has not been shown to predict response in other tumour types, such as breast<sup>[21,39]</sup> and cervical cancer<sup>[40]</sup>, with conflicting results seen in studies of head and neck squamous cell carcinomas<sup>[41,42]</sup>.

Future work is needed to accurately define at which time points a change in ADC from pre-treatment baseline values best correlate with tumour response and patient outcome for each cancer type and treatment. In one study, DWI was evaluated as a biomarker of tumour response in patients with locally advanced breast cancer undergoing neoadjuvant chemotherapy<sup>[43]</sup>. Although an increase in tumour ADC could be observed after the first cycle of treatment, the greatest sensitivity in differentiating responders from non-responders was seen after the third cycle.

### How?

Diffusion-weighted images are generated by applying a diffusion-sensitizing gradient, the strength of this gradient can be altered by changing the  $b$  value on the scanner. Higher  $b$  values indicate higher diffusion weighting, and the typical  $b$  values used for disease evaluation in the body vary between 0 and 1000 s/mm<sup>2</sup>. The technique can be implemented on most clinical MR systems at 1.5 and 3 T.

On a high  $b$  value (e.g. 1000 s/mm<sup>2</sup>) diffusion-weighted image, tumour tissue will usually appear brighter or show higher signal intensity compared with the native tissue from which it arises. Therefore, subjective assessment of tumour response can be made by reviewing tumour signal intensity on the high  $b$  value images before and after treatment. Tumour response is observed as signal reduction after treatment.

However, for more objective and consistent comparison of results, quantitative ADC measurement is desirable. The ADC map is automatically generated on a voxel-by-voxel basis on most scanners, and the value of each voxel describes the relationship between the logarithm of the signal intensity and the  $b$  value. The calculated ADC value is independent of magnetic field strength.

Solid, non-necrotic tumour tissues usually return low ADC values and effective treatment, as previously discussed, results in an increase in tumour ADC.

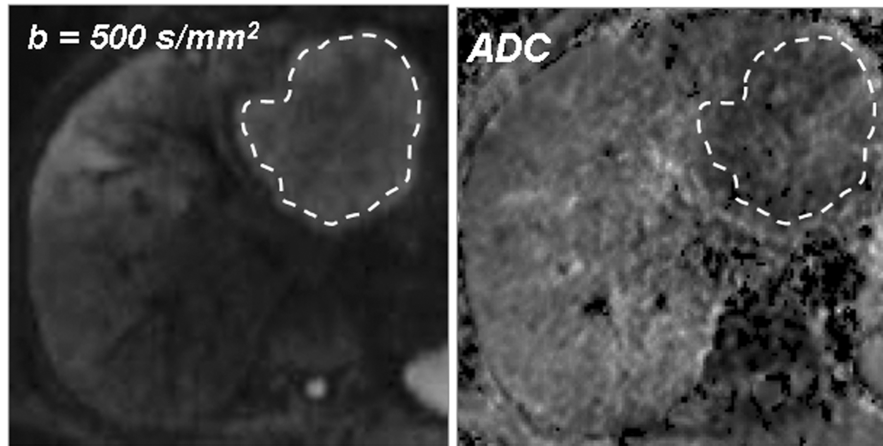


**Figure 6** ROI placement. An ROI is typically drawn just inside the outer border of a tumour on the high  $b$  value MR image and then copied onto the ADC map. This is because tumour borders are usually better delineated on the  $b$  value images compared with the ADC map.

To record tumour ADC values, a region of interest (ROI) is usually drawn to encompass the tumour of interest and the mean or median ADC value within the ROI recorded. ROIs can be manually drawn or by applying statistical region growing techniques available on some software. A few tips may be helpful with regards to ROI placement. First, as the tumour outline is usually better delineated on the high  $b$  value diffusion-weighted image compared with the ADC map, it is easier to mark out the tumour contour when the ROI is drawn on the  $b$  value image (Fig. 6). This ROI can then be copied and pasted onto the ADC map to record its value. Second, it may be desirable to draw the ROI just inside the outer border of the tumour to minimize any partial volume effects. Third, when comparing results before and after treatment, it is useful for the ROIs for both the pre-treatment and post-treatment scans to be drawn at the same sitting. This allows careful alignment of the images to match corresponding slice positions and ensure consistency in the approach to define the tumour contour. Fourth, although many studies have been performed using ADC results obtained at a single level through the tumour, it is worthwhile repeating ADC measurements at a few contiguous levels and then averaging the results to avoid sampling bias. Where available, the individual voxel values from each ROI can be pooled together, from which the mean or median ADC values of all the voxel evaluated can be derived. Last but not least, the choice of target lesion on which to perform ADC measurement should be made carefully and judiciously. The minimum lesion size amenable for ADC measurement should be at least twice the section thickness to avoid partial volume effects.

For tumours that exhibit considerable heterogeneity (e.g. mixed solid, necrotic and cystic), some authors have suggested using multiple ROIs to evaluate sub-regions within these tumours<sup>[44]</sup>. However, there may

be subjectivity and bias in such ROI placements. The use of other indices such as the minimum ADC ( $ADC_{\text{minimum}}$ ) within an ROI has also been advocated<sup>[45]</sup>. When considering the  $ADC_{\text{minimum}}$ , this should not be taken from an area with significant artefacts, as spuriously low values may be encountered<sup>[46]</sup>. One method of visualizing tumour heterogeneity is by evaluating the distribution of ADC values within a tumour using frequency histograms. Using special software, it may also be possible to map and observe the spatial distribution of specific ADC values within a lesion, providing a method to segment regions within a heterogeneous tumour by their ADC values.

More recently, functional diffusion maps, also known as parametric response maps, have been applied to detect early and heterogeneous tumour response to anticancer treatment (Fig. 7). This method of analysis is based on assessing ADC change for each imaging voxel within an ROI, relative to a threshold determined by the distribution of the pre-treatment ADC values (e.g. the 95% confidence limit of ADC distribution)<sup>[47,48]</sup>. In this way, the percentage of voxels within an ROI that have significantly increased above or decreased below the threshold after therapy can be determined. Studies using parametric response maps have been reported in brain gliomas, bone metastases, breast and head and neck cancers. It has been shown that parametric response maps can detect a significant drug effect even though the mean ADC value of a tumour does not change. Furthermore, it has been shown in patients with cerebral glioblastoma that an early response by parametric response maps was associated with better disease survival<sup>[49]</sup>. However, data analysis by parametric response maps requires excellent image registration between studies, to allow the same image voxels to be compared across time. This can be extremely challenging in the body, where motion and variations in the scan plane orientation between

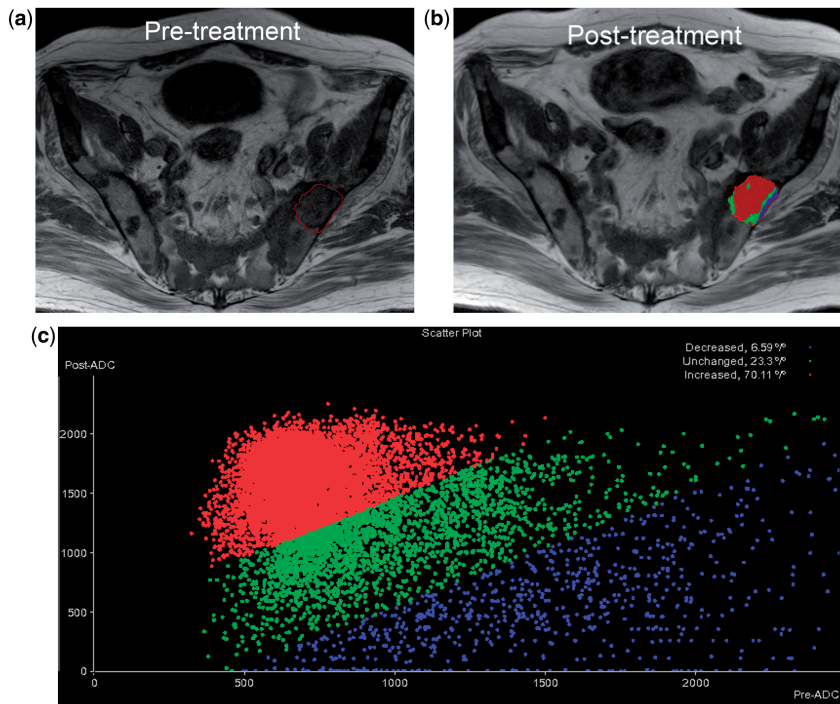


**Figure 7** Parametric response map. A 72-year-old man with metastatic prostate cancer. (a) Pre-treatment T1-weighted image of the pelvis showing extensive metastatic bone disease. A region of interest (in red) is drawn encompassing a metastasis in the left ilium. (b) Post-treatment T1-weighted image. Colours displayed within region of interest indicate voxels that show increase (red), decrease (blue) or no change (green) in ADC values relative to threshold determined by pre-treatment standard deviation of ADC values. (c) Scatter plot of ADC values on a voxel-by-voxel basis before and after treatment shows a large percentage of voxels showing increase in ADC values (in red) indicating treatment effects within tumour volume. (Maps generated using Oncotreat software, Siemens Medical system, Erlangen, Germany).

studies can make precise image registration difficult. Furthermore, tumours may shrink or grow between imaging studies, further confounding accurate registration of the pre- and post-treatment datasets.

## Challenges and future developments

There is now considerable interest in applying more sophisticated mathematical models to DWI data to extract quantitative parameters that reflect tissue microcapillary perfusion. By acquiring DWI images using multiple  $b$  values (typically 6 or more), the DWI data may be fitted using a biexponential mathematical model, such as one based on the principles of intravoxel incoherent motion (IVIM). Using such an approach, quantitative parameters that reflect vascular flow ( $f$  and  $D^*$ ) and tissue diffusivity ( $D$ ) can be derived. It is still unclear whether such an approach would improve the assessment of drug effects and further studies are warranted.

Although DWI is widely accepted in routine radiological practice in the brain, its role in extracranial disease continues to evolve. Many centres still do not use DWI as a standard imaging sequence. However, the increasing body of evidence for DWI as a promising tool for

monitoring and predicting disease response will undoubtedly see its more widespread implementation in future years. The issue of technical standardization within and across MRI platforms will need to be addressed to help DWI become standard practice. As software technology improves, better tools that streamline DWI data analysis should become progressively available. Advances in understanding of the evolution of tumour biology in response to treatment will help optimal timing of future studies.

## References

- [1] Miller AB, Hoogstraten B, Staquet M, *et al.* Reporting results of cancer treatment. *Cancer* 1981; 47: 207–14. doi:10.1002/1097-0142(19810101)47:1<207::AID-CNCR2820470134>3.0.CO;2-6.
- [2] Eisenhauer EA, Therasse P, Bogaerts J, *et al.* New response evaluation criteria in solid tumours: revised RECIST guideline (version 1.1). *Eur J Cancer* 2009; 45: 228–47. doi:10.1016/j.ejca.2008.10.026. PMID:19097774.
- [3] Therasse P, Arbuck SG, Eisenhauer EA, *et al.* New guidelines to evaluate the response to treatment in solid tumors. European Organization for Research and Treatment of Cancer, National Cancer Institute of the United States, National Cancer Institute of Canada. *J Natl Cancer Inst* 2000; 92: 205–16. doi:10.1093/jnci/92.3.205. PMID:10655437.



- [4] Harry VN, Semple SI, Parkin DE, *et al.* Use of new imaging techniques to predict tumour response to therapy. *Lancet Oncol* 2010; 11: 92–102. doi:10.1016/S1470-2045(09)70190-1.
- [5] Husband JE, Schwartz LH, Spencer J, *et al.* Evaluation of the response to treatment of solid tumours – a consensus statement of the International Cancer Imaging Society. *Br J Cancer* 2004; 90: 2256–60.
- [6] Choi H, Charnsangavej C, Faria SC, *et al.* Correlation of computed tomography and positron emission tomography in patients with metastatic gastrointestinal stromal tumor treated at a single institution with imatinib mesylate: proposal of new computed tomography response criteria. *J Clin Oncol* 2007; 25: 1753–9. doi:10.1200/JCO.2006.07.3049. PMID:17470865.
- [7] Young H, Baum R, Cremerius U, *et al.* Measurement of clinical and subclinical tumour response using [<sup>18</sup>F]-fluorodeoxyglucose and positron emission tomography: review and 1999 EORTC recommendations. European Organization for Research and Treatment of Cancer (EORTC) PET Study Group. *Eur J Cancer* 1999; 35: 1773–82. doi:10.1016/S0959-8049(99)00229-4.
- [8] Mazaheri Y, Shukla-Dave A, Hricak H, *et al.* Prostate cancer: identification with combined diffusion-weighted MR imaging and 3D 1H MR spectroscopic imaging – correlation with pathologic findings. *Radiology* 2008; 246: 480–8. doi:10.1148/radiol.2462070368. PMID:18227542.
- [9] Hricak H, Choyke PL, Eberhardt SC, *et al.* Imaging prostate cancer: a multidisciplinary perspective. *Radiology* 2007; 243: 28–53. doi:10.1148/radiol.2431030580. PMID:17392247.
- [10] Umbehr M, Bachmann LM, Held U, *et al.* Combined magnetic resonance imaging and magnetic resonance spectroscopy imaging in the diagnosis of prostate cancer: a systematic review and meta-analysis. *Eur Urol* 2009; 55: 575–90. doi:10.1016/j.eururo.2008.10.019. PMID:18952365.
- [11] Padhani AR, Leach MO. Antivascular cancer treatments: functional assessments by dynamic contrast-enhanced magnetic resonance imaging. *Abdom Imaging* 2005; 30: 325–42. doi:10.1007/s00261-004-0265-5. PMID:15688112.
- [12] Padhani AR, Liu G, Koh DM, *et al.* Diffusion-weighted magnetic resonance imaging as a cancer biomarker: consensus and recommendations. *Neoplasia* 2009; 11: 102–25.
- [13] Koh DM, Collins DJ. Diffusion-weighted MRI in the body: applications and challenges in oncology. *AJR Am J Roentgenol* 2007; 188: 1622–35. doi:10.2214/AJR.06.1403. PMID:17515386.
- [14] Koh DM, Scurr E, Collins D, *et al.* Predicting response of colorectal hepatic metastasis: value of pretreatment apparent diffusion coefficients. *AJR Am J Roentgenol* 2007; 188: 1001–8. doi:10.2214/AJR.06.0601. PMID:17377036.
- [15] Koh DM, Blackledge M, Collins DJ, *et al.* Reproducibility and changes in the apparent diffusion coefficients of solid tumours treated with combretastatin A4 phosphate and bevacizumab in a two-centre phase I clinical trial. *Eur Radiol* 2009; 19: 2728–38. doi:10.1007/s00330-009-1469-4. PMID:19547986.
- [16] Sasaki M, Yamada K, Watanabe Y, *et al.* Variability in absolute apparent diffusion coefficient values across different platforms may be substantial: a multivendor, multi-institutional comparison study. *Radiology* 2008; 249: 624–30. doi:10.1148/radiol.2492071681. PMID:18936317.
- [17] Chenevert TL, Stegman LD, Taylor JM, *et al.* Diffusion magnetic resonance imaging: an early surrogate marker of therapeutic efficacy in brain tumors. *J Natl Cancer Inst* 2000; 92: 2029–36. doi:10.1093/jnci/92.24.2029. PMID:11121466.
- [18] Pickles MD, Gibbs P, Lowry M, *et al.* Diffusion changes precede size reduction in neoadjuvant treatment of breast cancer. *Magn Reson Imaging* 2006; 24: 843–47. doi:10.1016/j.mri.2005.11.005. PMID:16916701.
- [19] Hein PA, Kremser C, Judmaier W, *et al.* Diffusion-weighted magnetic resonance imaging for monitoring diffusion changes in rectal carcinoma during combined, preoperative chemoradiation: preliminary results of a prospective study. *Eur J Radiol* 2003; 45: 214–22. doi:10.1016/S0720-048X(02)00231-0.
- [20] Takayama Y, Kishimoto R, Hanaoka S, *et al.* ADC value and diffusion tensor imaging of prostate cancer: changes in carbon-ion radiotherapy. *J Magn Reson Imaging* 2008; 27: 1331–5. doi:10.1002/jmri.21388. PMID:18504751.
- [21] Woodhams R, Kakita S, Hata H, *et al.* Identification of residual breast carcinoma following neoadjuvant chemotherapy: diffusion-weighted imaging – comparison with contrast-enhanced MR imaging and pathologic findings. *Radiology* 2010; 254: 357–66. doi:10.1148/radiol.2542090405. PMID:20093508.
- [22] Griffith JF, Yeung DK, Antonio GE, *et al.* Vertebral marrow fat content and diffusion and perfusion indexes in women with varying bone density: MR evaluation. *Radiology* 2006; 241: 831–8. doi:10.1148/radiol.2413051858. PMID:17053202.
- [23] Song I, Kim CK, Park BK, *et al.* Assessment of response to radiotherapy for prostate cancer: value of diffusion-weighted MRI at 3 T. *Am J Roentgenol* 2010; 194: W477–82. doi:10.2214/AJR.09.3557. PMID:20489065.
- [24] Mardor Y, Pfeffer R, Spiegelmann R, *et al.* Early detection of response to radiation therapy in patients with brain malignancies using conventional and high b-value diffusion-weighted magnetic resonance imaging. *J Clin Oncol* 2003; 2: 1094–100.
- [25] Hamstra DA, Galban CJ, Meyer CR, *et al.* Functional diffusion map as an early imaging biomarker for high-grade glioma: correlation with conventional radiologic response and overall survival. *J Clin Oncol* 2008; 20: 3387–94.
- [26] Hein PA, Kremser C, Judmaier W, *et al.* Diffusion-weighted magnetic resonance imaging for monitoring diffusion changes in rectal carcinoma during combined, preoperative chemoradiation: preliminary results of a prospective study. *Eur Radiol* 2003; 45: 214–22.
- [27] Kim SH, Lee JM, Hong SH, *et al.* Locally advanced rectal cancer: added value of diffusion-weighted MR imaging in the evaluation of tumor response to neoadjuvant chemo- and radiation therapy. *Radiology* 2009; 253: 116–25. doi:10.1148/radiol.2532090027. PMID:19789256.
- [28] Chen CY, Li CW, Kuo YT, *et al.* Early response of hepatocellular carcinoma to transcatheter arterial chemoembolisation: choline levels and MR diffusion constants – initial experience. *Radiology* 2006; 239: 448–56. doi:10.1148/radiol.2392042202. PMID:16569781.
- [29] Kamel IR, Reyes DK, Liapi E, *et al.* Functional MR imaging assessment of tumor response after 90Y microsphere treatment in patients with unresectable hepatocellular carcinoma. *J Vasc Interv Radiol* 2007; 18: 49–56. doi:10.1016/j.jvir.2006.10.005. PMID:17296704.
- [30] Batchelor TT, Sorensen AG, di Tomaso E, *et al.* AZD2171, a pan-VEGF receptor tyrosine kinase inhibitor, normalizes tumor vasculature and alleviates edema in glioblastoma patients. *Cancer Cell* 2007; 11: 83–95. doi:10.1016/j.ccr.2006.11.021. PMID:17222792.
- [31] Gerstner ER, Chen PJ, Wen PY, *et al.* Infiltrative patterns of glioblastoma spread detected via diffusion MRI after treatment with cediranib. *Neuro Oncol* 2010; 12: 466–72.
- [32] Schraml C, Schwenzer NF, Martirosian P, *et al.* Diffusion-weighted MRI of advanced hepatocellular carcinoma during sorafenib treatment: initial results. *Am J Roentgenol* 2009; 193: W301–7. doi:10.2214/AJR.08.2289. PMID:19770299.
- [33] DeVries AF, Kremser C, Hein P, *et al.* Tumor microcirculation and diffusion predict therapy outcome for primary rectal carcinoma. *Int J Radiat Oncol Biol Phys* 2003; 56: 958–65. doi:10.1016/S0360-3016(03)00208-6.
- [34] Dzik-Jurasz A, Domenig C, George M, *et al.* Diffusion MRI for prediction of response of rectal cancer to chemoradiation. *Lancet* 2002; 360: 307–8. doi:10.1016/S0140-6736(02)09520-X.
- [35] Sun YS, Zhang XP, Tang L, *et al.* Locally advanced rectal carcinoma treated with preoperative chemotherapy and radiation therapy: preliminary analysis of diffusion-weighted MR imaging for early detection of tumor histopathological downstaging.

- Radiology 2010; 254: 170–8. doi:10.1148/radiol.2541082230. PMID:20019139.
- [36] Oh J, Henry R, Pirkzall A, *et al.* Survival analysis in patients with glioblastoma multiforme: predictive value of choline-to-N-acetylaspartate index, apparent diffusion coefficient, and relative cerebral blood volume. *J Magn Reson Imaging* 2004; 19: 546–54. doi:10.1002/jmri.20039. PMID:15112303.
- [37] Moffat BA, Chenevert TL, Lawrence TS, *et al.* Functional diffusion map: a noninvasive MRI biomarker for early stratification of clinical brain tumour response. *Proc Natl Acad Sci U S A* 2005; 102: 5524–9. doi:10.1073/pnas.0501532102. PMID:15805192.
- [38] Cui Y, Zhang XP, Sun YS, *et al.* Apparent diffusion coefficient: potential imaging biomarker for prediction and early detection of response to chemotherapy in hepatic metastases. *Radiology* 2008; 248: 894–900. doi:10.1148/radiol.2483071407. PMID:18710982.
- [39] Nilsen F, Fangberget A, Geier O, *et al.* Diffusion-weighted magnetic resonance imaging for pretreatment prediction and monitoring of treatment response of patients with locally advanced breast cancer undergoing neoadjuvant chemotherapy. *Acta Oncol* 2010; 49: 354–60. doi:10.3109/02841861003610184. PMID:20397769.
- [40] Harry VN, Semple SI, Gilbert FJ. Diffusion-weighted magnetic resonance imaging in the early detection of response to chemoradiation in cervical cancer. *Gynecol Oncol* 2008; 111: 213–20. doi:10.1016/j.ygyno.2008.07.048. PMID:18774597.
- [41] Kato H, Kanematsu M, Tanaka O, *et al.* Head and neck squamous cell carcinoma: usefulness of diffusion-weighted MR imaging in the prediction of a neoadjuvant therapeutic effect. *Eur Radiol* 2009; 19: 103–9. doi:10.1007/s00330-008-1108-5. PMID:18641991.
- [42] King AD, Mo FK, Yu KH, *et al.* Squamous cell carcinoma of the head and neck: diffusion weighted MR imaging for prediction and monitoring of treatment response. *Eur Radiol* 2010; 23[Epub ahead of print].
- [43] Sharma U, Danishad KK, Seenu V, *et al.* Longitudinal study of the assessment by MRI and diffusion-weighted imaging of tumor response in patients with locally advanced breast cancer undergoing neoadjuvant chemotherapy. *NMR Biomed* 2009; 22: 104–13. doi:10.1002/nbm.1245. PMID:18384182.
- [44] Jiang ZX, Peng WJ, Li WT, *et al.* Effect of b value on monitoring therapeutic response by diffusion-weighted imaging. *World J Gastroenterol* 2008; 14: 5893–9. doi:10.3748/wjg.14.5893. PMID:18855990.
- [45] Chen Z, Ma L, Lou X, *et al.* Diagnostic value of minimum apparent diffusion coefficient values in prediction of neuroepithelial tumour grading. *J Magn Reson Imaging* 2010; 31: 1331–8. doi:10.1002/jmri.22175. PMID:20512884.
- [46] Lee EJ, Lee SK, Agid R, *et al.* Preoperative grading of presumptive low-grade astrocytomas on MR imaging: diagnostic value of minimum apparent diffusion coefficient. *AJNR Am J Neuroradiol* 2008; 29: 1872–7. doi:10.3174/ajnr.A1254. PMID:18719036.
- [47] Galbán CJ, Chenevert TL, Meyer CR, *et al.* The parametric response map is an imaging biomarker for early cancer treatment outcome. *Nat Med* 2009; 15: 572–6.
- [48] Hamstra DA, Chenevert TL, Moffat BA, *et al.* Evaluation of the functional diffusion map as an early biomarker of time-to-progression and overall survival in high-grade glioma. *Proc Natl Acad Sci U S A* 2005; 102: 16759–64. doi:10.1073/pnas.0508347102. PMID:16267128.
- [49] Tsien C, Galbán CJ, Chenevert TL, *et al.* Parametric response map as an imaging biomarker to distinguish progression from pseudoprogression in high-grade glioma. *J Clin Oncol* 2010; 28: 2293–9. doi:10.1200/JCO.2009.25.3971. PMID:20368564.